Energy-Optimal Hopping in Parallel and Series Elastic One-Dimensional Monopeds

Yevgeniy Yesilevskiy
Department of Mechanical Engineering,
University of Michigan,
Ann Arbor, MI 48109
e-mail: yevyes@umich.edu

Zhenyu Gan
Department of Mechanical Engineering,
University of Michigan,
Ann Arbor, MI 48109
e-mail: ganzheny@umich.edu

C. David Remy
Department of Mechanical Engineering,
University of Michigan,
Ann Arbor, MI 48109
e-mail: cdremy@umich.edu

In this paper, we examine the question of whether parallel elastic actuation or series elastic actuation is better suited for hopping robots. To this end, we compare and contrast the two actuation concepts in energy optimal hopping motions. To enable a fair comparison, we employ optimal control to identify motion trajectories, actuator inputs, and system parameters that are optimally suited for each actuator concept. In other words, we compare the best possible hopper with parallel elastic actuation to the best possible hopper with series elastic actuation. The optimizations are conducted for three different cost functions: positive mechanical motor work, thermal electrical losses, and positive electrical work. Furthermore, we look at three representative cases for converting rotary motor motion to linear leg motion in a legged robot. Our model featured an electric DC-motor model, a gearbox with friction, damping in the leg spring, and contact collisions. We find that the optimal actuator choice depends both on the cost function and conversion of motor motion to leg motion. When considering only thermal electrical losses, parallel elastic actuation always performs better. In terms of positive mechanical motor work and positive electrical work, series elastic actuation is better when there is little friction in the gear-train. For higher gear-train friction parallel elastic actuation is more economical for these cost functions as well. [DOI: 10.1115/1.4039496]

1 Introduction

Springs play a fundamental role in legged locomotion. In nature, elastic elements are used for energy storage, as return springs, and to cushion impacts [1]. Model-based analyses have shown that compliant legs can explain the dynamics of human walking and running [2], as well as a wide variety of quadrupedal gaits, including walking, trotting, tölting, and galloping [3,4]. In all these cases, elastic energy storage enables the recycling of energy and improves energetic economy. Cavagna et al. [5] and Blickhan [6] observed that during running gaits, animals conserve energy by having the body undergo an elastic bouncing motion. In human in-place hopping, for example, the majority of the energetic fluctuations are generated passively through elastic energy storage in muscles and tendons [7,8]. Motivated by these biological benefits, elastic elements have been incorporated successfully in robotic simulations, e.g., see Refs. [9] and [10], and in hardware prototypes, e.g., see Refs. [11–15].

In robotic hardware, the two primary ways of incorporating elasticity into legs are to place springs in parallel or in series with the actuation source (Fig. 1). In a parallel elastic actuator (PEA), the motor contracts and extends the entire leg and spring. The spring force and motor force, therefore, act additively. The motor inertia moves with the joint and is not isolated from impacts. In a series elastic actuator (SEA), the motor moves the proximal end of the spring. The motor force must overcome the spring force. The motor inertia does not directly add to the joint motion and is isolated from impacts. Both types of actuator have been implemented in prototypes, e.g., see Refs. [16] and [17]. Yet, to date, there is still no detailed understanding of the effect of each actuator type on the energetics and motion characteristics of legged systems. In particular, there is still disagreement about which actuator solution is more energetically economical.

There is a broad range of similar questions that essentially try to determine the benefits of discrete design choices. Can a compliant ankle joint in a robot's leg improve efficiency? Is a quadrupedal robot faster with a spine that is rigid or deformable? Is a set of swinging arms useful for robotic locomotion? These questions are fundamentally difficult to answer. One cannot simply swap a particular feature in a robotic implementation or robotic model and then compare the performances of the two different variations. This is because an optimal robot with one of the two variations will likely have to look and behave very differently than an optimal robot with the other. For example, a robot with PEA might require a different spring stiffness and a different transmission ratio than a robot with SEA, and the two actuator types might need very different ways to power their motion. If we keep the system parameters of the two robots identical or apply the same type of motion in both cases, we will implicitly bias the comparison to favor one variation over the other. After all, we are not interested in the question of whether a *certain* robot with a certain motion strategy and a certain choice of parameters performs better with one design variation or the other. We would like to know if the *best possible* robot, with the best possible set of parameters, and the best possible motion strategy can benefit from the design variation. To answer this question, we have to investigate optimal motion, optimal parameters, and optimal morphology at the same time. Due to the complexity of the problem, it is impossible to do this comparison by conducting an exhaustive search or an analytical evaluation. Instead, we propose to use trajectory optimization to find the best possible actuator inputs and motion trajectories while simultaneously optimizing the system parameters.

This approach extends upon existing morphological optimizations in legged robotics [18–21]. These past studies optimize parameters to optimally adapt a model to a particular task but do not use the technique to compare discrete designs. It also extends on existing discrete structural comparisons [22] by using trajectory optimization on a realistic motor model and including morphological parameters directly in the optimization. In particular, this technique has not been applied in previous studies comparing PEA and SEA. An initial comparison was conducted, for example, by James et al. [23], and found that PEA was more economical. Grimmer et al. [24], on the other hand, found SEA to be more economical for a model of a human ankle joint. The difference in the two studies likely stems from their comparisons of *particular*

Contributed by the Mechanisms and Robotics Committee of ASME for publication in the Journal of Mechanisms and Robotics. Manuscript received March 16, 2017; final manuscript received February 26, 2018; published online April 5, 2018. Assoc. Editor: Jun Ueda.

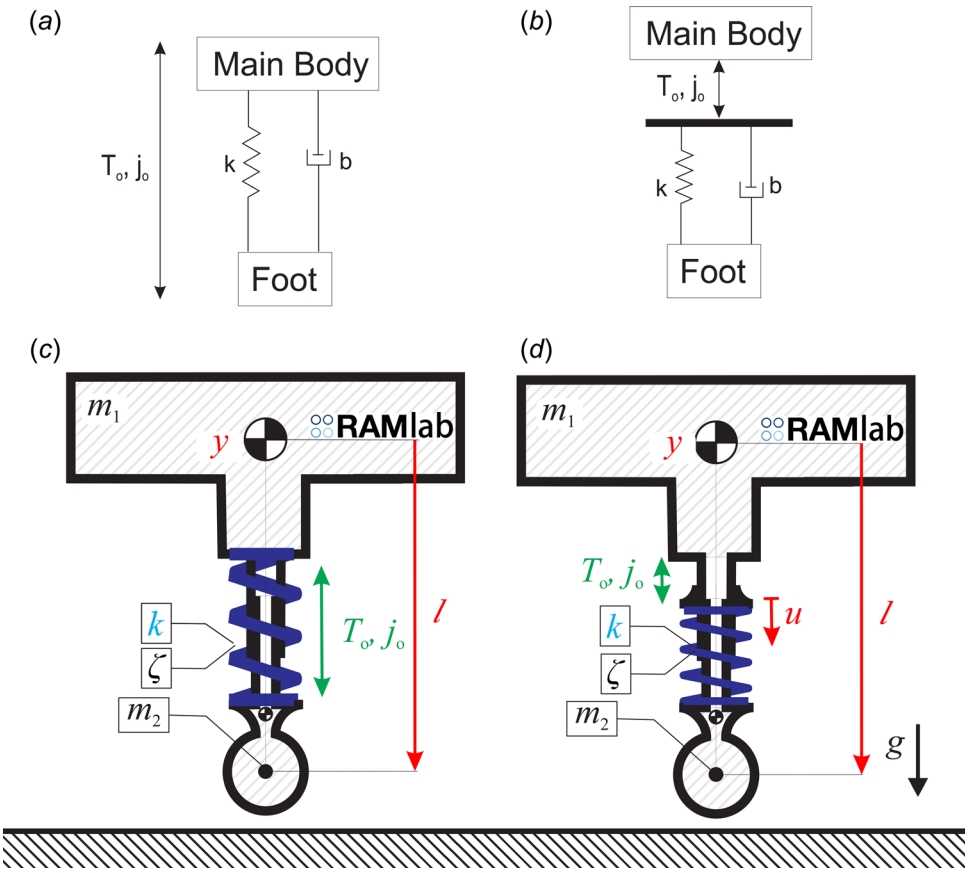

Fig. 1 This study investigated energetically optimal hopping motions for a one-dimensional (1D) hopper with either parallel elastic actuation (PEA, shown as schematic in (*a*) and detailed model in (*c*)) or series elastic actuation (SEA, (*b*) and (*d*)). For both hoppers we simultaneously optimized motion trajectories, actuator inputs, and actuation parameters for three different cost functions: positive mechanical motor work, thermal electrical losses, and positive electrical work. The optimization included main body position *y*, leg length *l*, motor position *u* (only for SEA), motor force after the transmission T_o, spring stiffness *k*, and rotary gearbox ratio n_r (not shown).

implementations of each actuator type, rather than the *best* implementation. Furthermore, the studies significantly simplified the problem. James et al. [23] only looks at a single cost function and a single set of parameters for actuator comparisons. Grimmer et al. [24] has similar simplifications, including ignoring the motor inertia and damping in the springs.

In this work, we performed a thorough comparison of PEA and SEA for the exemplary case study of in-place hopping. In a trajectory optimization framework, we considered inputs, motion trajectories, and system parameters simultaneously to understand their mutual effects and their full implications on the choice of PEA or SEA. As a basis for our study, we used a model that, while simple enough to lead to general conclusions, has enough detail to model more realistic motions during hopping, such as leg dynamics during flight. In particular, our models incorporated feet with mass, detailed electric DC motor models, damping in the springs, and gearbox friction. In addition, we enforced realistic constraints on the possible parameter values, motion trajectories, and motor inputs. We considered two different cases of rotary-to-linear transmissions that represent common values in modern legged robotics. We contrasted these two types with the more theoretical scenario of a completely frictionless transmission. Within each of these three cases, we examined a variety of cost functions quantifying work- and force-based efforts. We found that the optimal actuator type and motion was highly dependent on both the type of rotary to linear transmission as well as on the chosen cost function.

As hopping is highly relevant in legged locomotion, which often uses the template of a spring loaded inverted pendulum for bipedal [6] and multilegged [25] locomotion, our results are relevant for both a fundamental understanding of the effect of elastic actuators on legged motion as well as for applied hardware design. In addition to answering the question of which actuator type is better in different situations, our study provides a detailed understanding of what optimal motions look like and can, therefore, be used to "calibrate" trajectory optimization results in real hardware. To this end, the paper represents a culmination of our previous efforts analyzing optimal actuation [26–28].

2 Theoretical Discussion

In the past, discussions about which actuation concept is better suited for legged robotics often argued that PEA is better when minimizing motor torque and SEA is better when minimizing mechanical work, e.g., see Ref. [29]. To illustrate this argument and to use it as a departure point for our own work, we can formalize this distinction in terms of two different cost functions: the positive mechanical motor work C_{mech} (where the work done by the motor is equal to $T_m\omega_m$) and the thermal electrical losses C_{therm} (which is proportional to T_m^2). In these expressions, T_m is the torque created by the motor, and ω_m is the motor velocity. Since C_{therm} is only dependent on T_m, one could think that this cost function would indeed prefer PEA, where motor force and spring force act additively and the motor torque is thus reduced. SEA would be at a disadvantage, as its motor must actively provide the entire force acting on the leg. For C_{mech}, the situation is reversed. For SEA, the motor and main body components are well

insulated from impacts, and the inertia of the motor does not add directly to the joint motion, potentially leading to reduced mechanical losses. PEA seems to be at a disadvantage, as the rotor inertia now factors into collisions.

Upon closer inspection, however, the situation is not so clearly delineated. For each actuator type, adaptations in the hardware and in the motion strategy can alleviate the respective disadvantages. To illustrate the effects of different parameters and motion strategies, let us examine the simplified case of (nearly) loss-less hopping. To this end, we consider a hopper model with no foot mass and no damping in the springs. This hopper is driven by a motor with a rotor inertia of j_m that is connected to the joint via a frictionless gearbox with transmission ratio n. For both the PEA and SEA version of this hopper, we can, in fact, find entirely loss-less solutions for *both* cost functions. PEA can achieve $C_{\text{mech}} = 0$ by having the motor input no torque ($T_m = 0$) and, therefore, having the spring perform the hopping task passively. With this motion strategy, the only possible source of mechanical losses is collision losses in the rotor inertia

$$E_{\text{p,mc}} = \frac{1}{2}\left(\frac{j_o m_1}{m_1 + j_o}\right) \cdot v_{\text{foot}}^2 \tag{1}$$

where m_1 is the main body mass and v_{foot} represents the velocity of the foot at touchdown [26]. The reflected rotor inertia of the motor j_o scales with the square of the transmission ratio n: where we assume that the transmission ratio converts rotary to linear motion, giving j_o units of mass. By setting $n = 0$ and thus $j_o = 0$, the collision losses can be completely removed, which leads to $C_{\text{mech}} = 0$. There are no disadvantages to this choice, since no torque is required from the motor. This strategy also achieves $C_{\text{therm}} = 0$, as $T_m = 0$. In contrast, SEA can yield $C_{\text{mech}} = 0$ by setting $\omega_m = 0$. This fixes the location of the proximal end of the spring, letting the spring perform the hopping task entirely passively. Since in SEA, the rotor inertia is decoupled from the motion, no losses occur and the motion is periodic. This solution, however, requires a nonzero force to keep the motor in place as the leg spring compresses. In order to achieve $C_{\text{therm}} = 0$, SEA must, thus, set the transmission n to infinity. Since $T_o = nT_m$, where T_o is the output torque after the gearbox, C_{therm} is proportional to T_o^2/n^2. Using $n = \infty$ yields $C_{\text{therm}} = 0$. Again, there are no disadvantages to this choice, since no motion is required from the motor.

Even though the model in this analysis is a contrived example, it shows two important issues. First, with the right choice of motion and parameters, PEA and SEA can achieve the same performance for *both* work-based and torque-based cost functions. No actuator type is better per se. Second, the two actuator types require almost diametrically different strategies and parameters. PEA applies no force as the motor moves with the spring and utilizes a transmission ratio of $n = 0$. Choosing the opposite extreme of $n = \infty$ drives C_{therm} to infinity, as the collision losses in the motor become infinite. SEA keeps the motor at rest and requires a transmission ratio of $n = \infty$. If SEA were to choose the opposite extreme of $n = 0$ then C_{therm} would be driven to infinity, as it would take an infinite T_m to keep the motor still. It is clear that when trying to answer the question of which actuator type is better, we need to take into account that each actuator requires substantially different motion strategies and parameters.

The extreme values for n in this example are a consequence of the assumption that the hopping is otherwise lossless. As soon as we introduce damping and collision losses, these transmission values become extremely nonoptimal. When the motors must move and apply torques to do positive mechanical work to replace the inevitable energetic losses, finite nonzero transmission values n are necessary. In particular, SEA can no longer have an infinite n, as the resulting infinite reflected rotor inertia would require an infinite T_m to move the motor to replenish losses, which will drive both cost functions to infinity. PEA can also no longer have $n = 0$, as it will take an infinite T_m to transmit force through the gearbox and add energy to the system. That infinite T_m will again drive both cost functions to infinity. The infinite costs at both extremes of n suggest that there exist optimal choices for n in between. For a simplified SEA hopper, for example, such an optimal value has been derived analytically in Ref. [28]. Similar types of dependencies likely exist for other parameters and must be resolved by including the parameters in an optimization formulation.

Furthermore, there exist a number of complex relationships between optimal parameter choices and motion strategies. For example, for an actuator with PEA, one strategy would be to let the leg oscillate freely during flight ($T_m \approx 0$), which minimizes T_m and thus C_{therm}. Moreover, this oscillation can be timed such that the foot has zero velocity at touchdown, leading to no collision losses even in the presence of a foot mass. This timing is achieved by tuning the natural frequency f of the leg spring

$$f = \sqrt{\frac{k}{m_2 + j_o}} \tag{2}$$

which depends on the choice of stiffness k, transmission ratio n, and foot mass m_2. That is, through this natural dynamic oscillation, the choice of motion and parameters is coupled. Such an exploitation of natural dynamics can happen in a variety of ways and must, thus, be accounted for when trying to answer the question of which actuator type is more economical.

The main takeaway of these considerations is that motion and optimal morphology are strongly coupled and will differ greatly between hoppers with PEA and SEA. In order to figure out which actuator type is better, we have to investigate optimal motion and optimal morphology at the same time, such that we can compare the best possible SEA robot to the best possible PEA robot. In addition to the examples mentioned earlier, this question is even further complicated by the presence of friction in the gearbox and limits on the motor force and joint motion. With torque inputs, motion trajectories, system parameters, and limits mutually affecting each other in such complex ways, numerical optimization is the only suitable tool to understand the full implications of the choice of PEA or SEA.

3 Methods

In this paper, we used trajectory optimization to find the most energetically economical motions and parameters for each actuator configuration and used these optimal results as a basis for comparison. In particular, we examined optimal, periodic, one-dimensional, in-place hopping, and studied a variety of cost functions in a model-based approach. To this end, we established parametrized models of electrically driven PEA and SEA hoppers that included a dynamical model, a motor model, a detailed transmission model, and realistic limitations on all states and parameters. In this section, we outline these models, discuss our parameter choices, describe the cost functions, and detail our optimization approach. To minimize the number of free parameters in our analysis, all states and parameters were normalized with respect to total mass m_o, uncompressed leg length l_o, and gravity g.

3.1 Dynamical Model. Our study was based on the simple model of a hopper (Fig. 1). The hopper consisted of a main body with mass m_1 and a point foot segment with mass m_2. The motion of the hopper was restricted to a pure vertical movement; i.e., hopping in place. Its state was defined by the position and velocity of the main body (given by y and $\dot{y}$) and the length and contraction velocity of the leg (l and $\dot{l}$). The motion of the foot was coupled to the main body by a spring with stiffness k and damping ratio ζ. Having damping in the springs and a foot with mass meant that the system was energetically nonconservative. As a result, positive network had to be performed over the course of a stride. This work was created by an electric DC motor with an attached

transmission that produced a torque of T_o and had a reflected inertia of j_o. The mass of the motor is included as part of m_1. This actuator was either connected in parallel to the spring (PEA) or in series with the spring (SEA). During flight, the motion of the hopper was governed by the equations of motion $\mathbf{M}\ddot{\mathbf{q}} = \mathbf{h} + \boldsymbol{\tau}$, with the mass matrix $\mathbf{M}$, the gravitational terms $\mathbf{h}$, and the generalized forces $\boldsymbol{\tau}$.

For PEA, the motor was mounted in parallel to the spring, such that the leg force, F, was the sum of the force in the spring and the motor force

$$F = k(\ell_o - \ell) - b\dot{\ell} + T_o \tag{3}$$

The damping coefficient of the spring b was computed from the damping ratio ζ

$$b = 2\zeta\sqrt{km_2} \tag{4}$$

Since motor motion and leg motion were coupled, the vector of generalized coordinates $\mathbf{q}_{\text{PEA}} = (y, \ell)^{\text{T}}$ was only two-dimensional. The reflected rotor inertia j_o acted along the coordinate of ℓ, which led to the following mass matrix for PEA:

$$\mathbf{M}_{\text{PEA}} = \begin{bmatrix} m_1 + m_2 & -m_2 \\ -m_2 & m_2 + j_o \end{bmatrix} \tag{5}$$

The system was driven by the generalized forces $\boldsymbol{\tau}_{\text{PEA}} = (0, F)^{\text{T}}$. The differentiable force vector was given by $\mathbf{h}_{\text{PEA}} = (-(m_1 + m_2)g, m_2 g)^{\text{T}}$.

In the SEA case, the spring was rigidly attached to the foot on one end and attached to the motor transmission on the other. An additional pair of states (u and $\dot{u}$) described the position of the proximal end of the spring (coordinate origins were defined such that for $u = 0$, and an uncompressed spring, the leg length ℓ was equal to the resting length ℓ_o). The generalized coordinate vector, thus, had three components: $\mathbf{q}_{\text{SEA}} = (y, \ell, u)^{\text{T}}$. Since the motor was in series with the spring, the leg force, F, was equal to the force produced by the spring

$$F = k(u + \ell_o - \ell) + b(\dot{u} - \dot{\ell}) \tag{6}$$

The mass matrix for this system was given by

$$\mathbf{M}_{\text{SEA}} = \begin{bmatrix} m_1 + m_2 & -m_2 & 0 \\ -m_2 & m_2 & 0 \\ 0 & 0 & j_o \end{bmatrix} \tag{7}$$

The system was driven by the generalized forces $\boldsymbol{\tau}_{\text{SEA}} = (0, F, T_o - F)^{\text{T}}$. The differentiable force vector was given by $\mathbf{h}_{\text{SEA}} = (-(m_1 + m_2)g, m_2 g, 0)^{\text{T}}$.

For both models, the main body velocity and the leg retraction rate were equal during ground contact ($\dot{y} = \dot{\ell}$). That led to the modified equations of motion of $\ddot{y} = \ddot{\ell} = F/(m_1 + j_o) - m_1 g/(m_1 + j_o)$ for PEA and $\ddot{y} = \ddot{\ell} = (F/m_1) - g$ for SEA. This constraint implies that at the moment of touch-down, a collision brought the foot velocity $v_{\text{foot}} = \dot{y} + \dot{\ell}$ to zero.

3.2 Motor and Transmission Model. Since we were interested in the realistic trade-offs between thermal losses and mechanical work within each of the actuation concepts, we included a model of an electric DC motor in our simulation [30]. To simplify the analysis, we neglected the electrical dynamics due to the winding inductance. The motor torque is related linearly to the electrical motor current i via the motor torque constant k_T ($T_m = ik_T$). The thermal losses in the motor are given by

$$P_{\text{therm}} = i^2 R = \frac{T_m^2}{k_T^2} R = \frac{T_m^2}{k_T k_b} R = \frac{T_m^2}{K} \tag{8}$$

where R is the armature resistance, k_b is the motor speed constant, and K is the speed torque gradient of the motor. Here, we made use of the fact that in SI units, $k_T = k_b$.

The motor rotor had an inertia of j_m and was modeled to be connected to a transmission system. This transmission had two roles. First, it amplified the motor torque ($T_o = nT_m$), while reducing the output speed ($\omega_o = (1/n)\omega_m$). Second, it converted the rotational motion of the motor to a linear motion that allowed the hopper's leg to extend and contract. We defined the overall transmission as the combination of a rotary gearbox with transmission ratio n_r (a unitless quantity), and a rotary to linear transmission with transmission ratio n_ℓ (with normalized units of rad/ℓ_o). The overall transmission ratio n was given by the product of $n_r n_\ell$. For simplicity, we neglected the inertia associated with the transmission, assuming that the inertia of the actuator is dominated by the reflected inertia of the rotor

$$j_o = (n_r n_\ell)^2 j_m \tag{9}$$

We considered two representative values used for converting rotary to linear motion in modern legged robotics: a large value of $n_\ell = 200\,\text{rad}/\ell_o$ and a small value of $n_\ell = 2\,\text{rad}/\ell_o$.

These values for n_ℓ were chosen because they are roughly representative of the transmission given by a ball screw [31] and a knee joint bent at approximately 45 deg, respectively. For both cases, for simplicity, we considered n_ℓ to be a frictionless transmission. This is evident for the knee joint and good approximation for the ball screw, which can have an efficiency of torque conversion of 90% and higher [31]. The only source of transmission friction was, thus, in the rotary gearbox n_r. This was an important consideration. A particular choice of n_ℓ may be able to better avoid n_r frictional losses. We modeled these n_r losses as being created by a planetary gearbox with dry friction. The torque output after the transmission is, therefore, given by

$$T_o = n_\ell(n_r T_m - \text{sign}(\omega_m) T_f) \tag{10}$$

where T_m is the torque output by the motor, ω_m is the motor speed, and T_f is the coulomb frictional torque of the gearbox. We calculated T_f in Eq. (10) from the maximum gearbox torque conversion efficiency ε_{max}

$$\varepsilon_{\text{max}} = \frac{T_{\text{o,max}}}{T_{\text{o,max}} + n_\ell T_f} \tag{11}$$

where $T_{\text{o,max}}$ is the maximum continuous output torque. Substituting into Eq. (10) and rearranging yields

$$T_f = T_{\text{o,max}} \frac{(1 - \varepsilon_{\text{max}})}{n_\ell \varepsilon_{\text{max}}} \tag{12}$$

For comparison, we included a third case in our analysis which assumed a completely frictionless transmission system (with $\varepsilon_{\text{max}} = 1$). This was done to understand which transmission choices would be optimal in the absence of any penalty associated with larger gearbox friction. Since in this frictionless case, there is no difference between n_ℓ and n_r; we simply set $n_\ell = 1$.

3.3 Model Parameters. We found all necessary motor parameters by applying logarithmic regression to data from 132 Maxon motors in the RE and EC series [32]. We found that

$$K \approx 0.00567(m_m)^{1.80}\ 1/\text{N m s} \tag{13}$$

$$j_{\text{rot}} \approx 2.85 \times 10^{-05}(m_m)^{1.72}\ \text{kg m}^2 \tag{14}$$

$$T_{\text{m,max}} \approx 0.570(m_m)^{1.20}\ \text{N} \cdot \text{m} \tag{15}$$

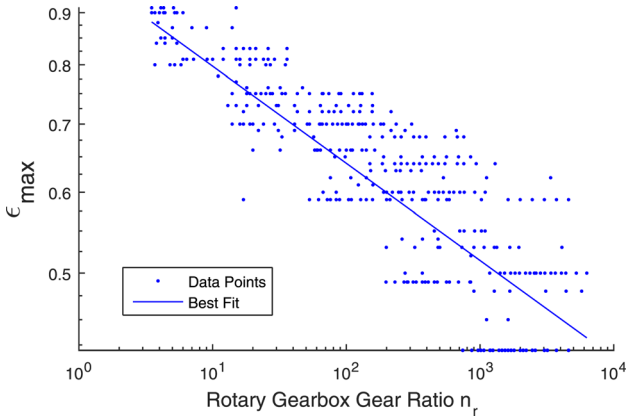

Fig. 2 The logarithmic regression of the maximum torque conversion efficiency of the rotary gearbox ε_{max} as a function of the rotary gearbox gear ratio n_r. The regression was based on 809 gearboxes [32].

$$\omega_{\mathrm{m,max}} \approx 1350(m_m)^{-0.182}\,1/\mathrm{s} \tag{16}$$

where m_m is the mass of the motor in kg, $T_{m,\max}$ is the maximum motor torque,[1] and $\omega_{m,\max}$ is the maximum permissible speed of the motor. Note that the values in these equations are not yet normalized.

We modeled the maximal efficiency to scale exponentially with the gear ratio n_r by the exponent γ. This decision was motivated by the observation that gear ratio scales approximately exponentially with stage number, which, in turns, scales approximately linearly with efficiency [32]. Our efficiency estimate was based on a logarithmic regression over 809 gearboxes from a major motor and gearbox manufacturer [32]. The results of the regression are shown in Fig. 2. We found that

$$\varepsilon_{\max} \approx 0.993(n_r)^{-0.0952} \approx 1(n_r)^{-0.0952} = n_r^{\gamma} \tag{17}$$

where the final approximation ensured that the efficiency was 100% when there was no gearbox ($n_r = 1$).

We assumed that the gearbox was appropriately chosen to be able to handle the maximum motor torque. As a result, we calculated the maximum continuous output torque after the transmission, $T_{\mathrm{o,max}}$, by

$$T_{\mathrm{o,max}} = n_r n_\ell T_{\mathrm{m,max}} \tag{18}$$

All parameters and their limits are reported in Table 1. They are based off of our previous hardware [33], as done in Ref. [28]. In particular, we chose a value of $m_m = 0.6\,\mathrm{kg}$, $m_o = 5\,\mathrm{kg}$, and $\ell_o = 0.4\,\mathrm{m}$.

3.4 Cost Functions. To measure the energetic efficiency of each actuation variation, we used three cost functions: positive mechanical motor work, thermal electrical losses, and positive electrical work. All cost functions are expressed as an integral over a single hop, from time $t = 0$ until $t = T$.

3.4.1 Positive Mechanical Motor Work. The positive mechanical motor work refers to the positive mechanical work that is performed by the motor. In a periodic motion, it is equivalent to the sum of the damping losses, collision losses, negative motor work, and frictional losses in the gearbox. The positive motor work is defined as

$$C_{\mathrm{mech}} = \int_0^T \max(T_m\omega_m, 0)dt \tag{19}$$

3.4.2 Thermal Electrical Losses. The thermal electrical losses cost function expresses the i^2R losses in the motor windings. It is given by

$$C_{\mathrm{therm}} = \int_0^T \frac{T_m^2}{K}dt \tag{20}$$

3.4.3 Positive Electrical Work. Positive electrical work is the integral of the positive electrical power used by the motor. It combines mechanical work and thermal losses. The positive electrical work is equal to

$$C_{\mathrm{el}} = \int_0^T \max\left(T_m\omega_m + \frac{T_m^2}{K}, 0\right)dt \tag{21}$$

As in Ref. [28] we assumed that the robot was unable to recover negative electrical work and store it. Negative motor work could be used, however, to compensate for thermal losses. This cost function provides a close approximation of the total energy discharge from a battery that would be required to power the motors.

3.5 Trajectory Optimization. For these models and cost functions, energy efficient motions were generated via trajectory optimization using a multiple shooting approach. To this end, we analyzed motions from apex transit to apex transit and enforced periodic boundary conditions to simulate a continuous hopping motion. The optimization problem can be formulated mathematically as

$$\min_{T,T_m,\mathbf{q},\dot{\mathbf{q}},k,n_r} C(\mathbf{q},\dot{\mathbf{q}},T_m) \tag{22}$$

$$\begin{aligned}
&\text{subject to:}\\
&\mathbf{M}\ddot{\mathbf{q}} = \mathbf{h} + \boldsymbol{\tau}\\
&\mathbf{q}(0) = \mathbf{q}(T)\\
&y(T) = 1.3\ell_0\\
&u_{\min} < u(t) < u_{\max}\\
&\ell_{\min} < \ell(t) < \ell_{\max}\\
&-T_{\mathrm{m,max}} < T_m(t) < T_{\mathrm{m,max}}\\
&-\omega_{\mathrm{m,max}} < \omega_m(t) < \omega_{\mathrm{m,max}}\\
&k_{\min} < k < k_{\max}\\
&n_{\mathrm{r,min}} < n_r < n_{\mathrm{r,max}}
\end{aligned} \tag{23}$$

A hopping height of $y(T) = 1.3\ell_0$ was chosen to ensure that the hoppers had a flight phase. All bounds are given in Table 1. The motor torque $T_m(t)$ was parametrized as a piecewise linear function. The aforementioned optimization problem was implemented in the optimization package MUSCOD, which utilizes a fourth/fifth-order Runge–Ketta–Fehlberg numerical integration algorithm [34–36]. We tried multiple initial conditions, all leading to the same results.

Note that the gearbox gear ratio n_r and the spring stiffness k were free parameters in the optimization. System properties that were unrelated to the actuator configuration were left fixed. These parameters included the masses (m_1 and m_2) and the damping ratio ζ.

In order to obtain a system that behaved better numerically, we approximated discontinuities in the cost functions (as has been done, for example, by Srinivasan and Ruina [37]). In particular, we smoothed the $\max(0, x)$ function using the following equation:

[1]This value is twice the maximum continuous torque the motor can provide. It is the maximum value suggested through personal communication with Maxon Motor.

Table 1 Model parameters and bounds expressed with respect to total mass m_o, leg length l_o, and gravity g

$m_1 = 0.95\ m_o$	$u_{\min} = -0.15\ \ell_0$	$n_{r,\min} = 1$
$m_2 = 0.05\ m_o$	$u_{\max} = 0.15\ \ell_0$	$n_{r,\max} = 6285$
$\zeta = 0.2$	$k_{\min} = 0.0001\ m_o g/\ell_o$	$\ell_{\min} = 0.5\ \ell_0$
$\ell_{\max} = 1.15\ \ell_0$	$k_{\max} = 1000\ m_o g/\ell_o$	$K = 2.3 \times 10^{-04}\ 1/m_o\sqrt{g\ell_o}$
$j_{\text{rot}} = 1.48 \times 10^{-05}\ m_o \ell_o^2$	$T_{m,\max} = 0.0157\ m_o g \ell_o$	$\omega_{m,\max} = 748\ \text{rad}\sqrt{g/\ell_o}$

$$\max(0, x) \approx \sigma \log\left(1 + e^{\frac{x}{\sigma}}\right) \tag{24}$$

with $\sigma = 0.001$. We also smoothed the function $\text{sign}(\omega_m)$ using the following equation:

$$\text{sign}(\omega_m) \approx \frac{2}{1 + e^{-\alpha\omega_m}} - 1 \tag{25}$$

with $\alpha = 100$.

4 Optimal Configurations, Motions, and Parameters

As a result of the optimization-based motion generation and parameter identification, we found that the ideal actuator type was both dependent on the choice of rotary to linear transmission and on the selected cost function. For positive electrical work, which combines mechanical motor work with thermal losses and reflects a realistic trade-off between these two contributions, we found that SEA was the optimal actuator type for an ideal, frictionless transmission as well as for the $n_\ell = 200\,\text{rad}/\ell_o$ case. For a hopper with $n_\ell = 2\,\text{rad}/\ell_o$, PEA was the optimal actuator type (Fig. 3). In the following, we elaborate on the optimal actuator type for each configuration and detail the resulting motion profiles and parameter choices for each case.

4.1 Frictionless Transmission. For a completely frictionless transmission, the energetically optimal actuator type depended on the cost function (Fig. 4). For positive mechanical motor work C_{mech}, the SEA hopper was 67% more energetically economical than PEA (0.070 $m_o g \ell_o$ versus 0.14 $m_o g \ell_o$). For both actuator types, energy was primarily lost to damping, accounting for 85% of C_{mech} for SEA and 96% for PEA. In terms of thermal electrical losses C_{therm}, the PEA hopper was 72% more economical than SEA (0.017 $m_o g \ell_o$ versus 0.036 $m_o g \ell_o$). For the electrical work C_{el} the SEA hopper was 75% more energetically economical than PEA (0.12 $m_o g \ell_o$ versus 0.25 $m_o g \ell_o$). For both actuator types, the C_{el} cost was primarily caused by damping and thermal losses in the spring and motor. Negative mechanical motor work was negligible, indicating a preference for following the natural dynamics of the system and exploiting passive storage of excess energy.

When optimizing for C_{mech} and C_{therm} individually, the results can largely be explained by the inherent advantages of each actuator type. SEA's advantage when optimizing for C_{mech} stemmed from the fact that SEA can directly influence the relative rate of spring motion and therefore decrease damping losses. For example, during the second half of stance, the actuator u is pushed downwards to inject energy but also to reduce the extension rate of the spring (as discussed in Ref. [38]). Such a strategy is not possible for PEA during stance where the spring motion is inherently coupled to the main body motion. PEA can reduce damping losses during flight, however, by holding the leg at its maximum length. This strategy reduces the effective hopping height and avoids oscillations with their associated damping losses in the air. Additionally, the foot is released slightly before touchdown to have its relative velocity with the ground be approximately zero (i.e., the leg velocity $\dot{\ell}$ approximately matched the main body velocity $\dot{y}$), minimizing collision losses (we will refer to this as the *clamping strategy*). As for minimizing C_{therm}, the main advantage of PEA stemmed from the fact that PEA did not need to support the weight of the robot, which reduced the required motor forces. Furthermore, the parameters for spring stiffness and gear ratio were tuned precisely such that when the leg oscillated nearly freely during flight (without any large peaks in the motor torque T_m) the leg velocity, $\dot{\ell}$ approximately matched the main body velocity at touchdown (we will refer to this as the *oscillation strategy*), which again minimized collision losses (Fig. 5).

What is surprising is that the rather small margins for each of these two cost functions turned into a large benefit for SEA in the combined cost function of positive electrical work C_{el}. This clear advantage of SEA can be explained by the fact that the optimal motion profiles for C_{mech} and C_{therm} were very similar (Fig. 5). The motor trajectory held the leg length nearly constantly at its maximum extension during flight and injected energy into the

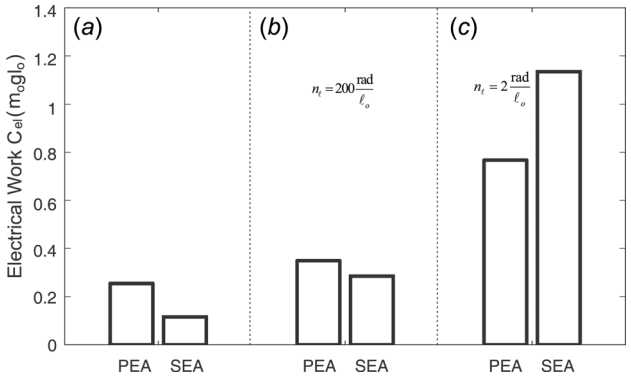

Fig. 3 The optimal positive electrical work values at a hopping height of $h = 1.3\ell_o$. Three cases are shown: a theoretical entirely frictionless transmission, a rotary to linear transmission of $n_\ell = 200\,\text{rad}/\ell_o$ with a rotary gearbox with friction, and a rotary to linear transmission of $n_\ell = 2\,\text{rad}/\ell_o$ with a rotary gearbox with friction. SEA is the most energetically economical choice for both the frictionless transmission and $n_\ell = 200\,\text{rad}/\ell_o$ cases. PEA is better for the $n_\ell = 2\,\text{rad}/\ell_o$ case. (*a*) frictionless transmission, (*b*) rotary gearbox with friction, frictionless $n_l = 200\ \text{rad}/\ell_o$, and (*c*) rotary gearbox with friction, frictionless $n_l = 200\ \text{rad}/\ell_o$.

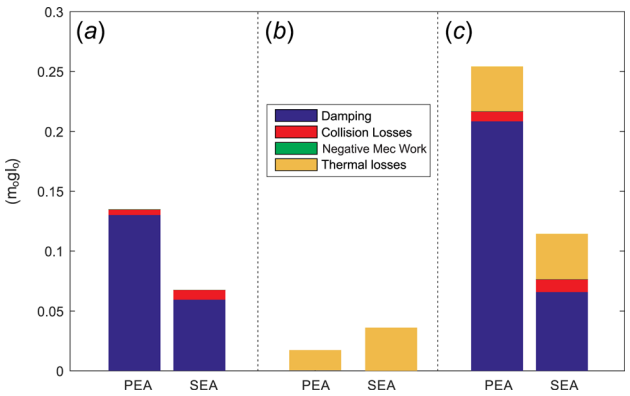

Fig. 4 An energetic breakdown is shown for the three cost functions in the case of a frictionless transmission. For both the positive mechanical motor work and the positive electrical work, SEA is the energetically optimal actuator type. For thermal losses, PEA is the optimal actuator type. (*a*) C_{mech}, (*b*) C_{therm}, and (*c*) C_{el}.

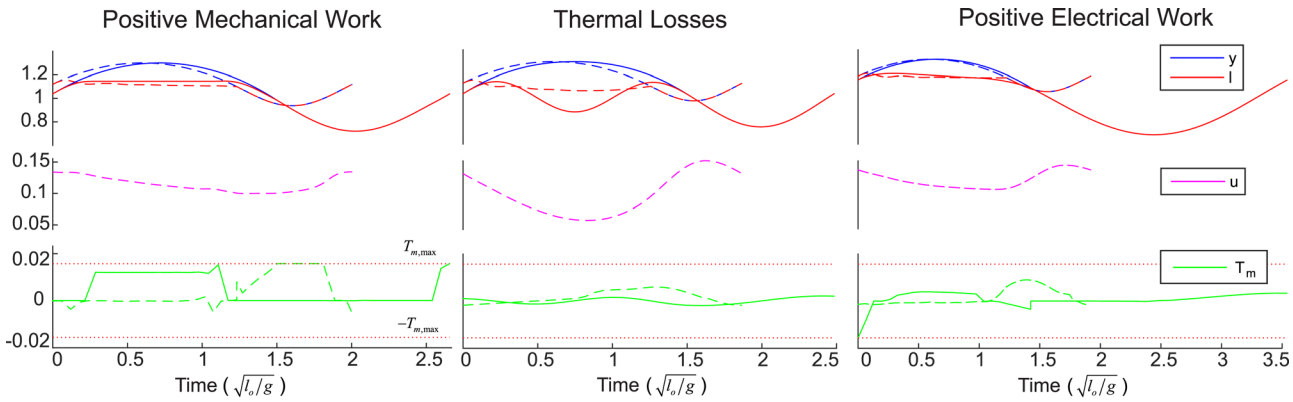

Fig. 5 Optimal motions and actuator inputs for the frictionless transmission. Shown are the results for optimizations based on positive mechanical motor work, thermal losses, and electrical work. The leg motion for SEA (dashed line) is very similar for all cost functions. In contrast, for PEA (solid line), the leg motion is drastically different when optimized for positive mechanical motor work as compared to thermal losses. As a result, when positive mechanical motor work and thermal losses are combined into a single cost function, the electrical work, PEA must trade-off between two very different motion strategies.

system during stance. It was, therefore, easy for SEA to find a strategy that could keep both C_{mech} and C_{therm} small at the same time when optimizing for C_{el}. The total C_{el} effort is merely a sum of the individual cost functions (Fig. 4). For PEA, in contrast, the motion trajectory differed significantly depending on the chosen cost function. For C_{mech}, the motion of the leg was similar to SEA, utilizing the clamping strategy; whereas for C_{therm}, the optimal motion is the oscillation strategy. For the combined cost function C_{el}, PEA, therefore, had to resolve a severe trade-off between two very different actuation strategies. As a result, for C_{el}, PEA had both higher mechanical work (primarily driven by an increase in damping losses) and higher thermal losses than for either C_{mech} or C_{therm}.

The aforementioned flight motion strategies indicate an important difference between our modeling and previous modeling efforts. The presence of foot mass and actuator inertia in our model allows us to present these optimal actuation strategies during the flight phase. Those strategies differ, for example, from those presented in Refs. [9], [39], and [40] which, due to their massless foot, only look at forces during the stance phase. Furthermore, having massless feet, and no damping, as the aforementioned papers do, allows for entirely lossless hopping strategies. For example, Alexander [9] states that for a SEA "it is possible to find a running gait that requires no work from the telescopic actuators, for any combination of speed and stride length." For PEA, the same can be said. Without collision losses or damping, the spring can passively store and replace all of the energy during hopping. Having both cases be entirely lossless would make a comparison of the two types of actuators impossible, and therefore justifies the added complexity of our model.

For all cost functions, the optimal PEA hopper had a significantly lower transmission ratio $n = n_r n_l$ than SEA (Table 2). Smaller values for n are better for PEA, because the reflected rotor inertia directly adds to the collision losses (Eq. (1)). Since the spring force and motor torque act additively for PEA, the output

Table 2 Optimal stiffness and transmission values for the frictionless transmission. Here, n is the overall transmission ratio ($n = n_r n_\ell$).

Cost function	Actuator type	k ($m_o g/\ell_o$)	n (rad/ℓ_o)
Positive motor work C_{mech}	PEA	27.5	41.0
Positive motor work, C_{mech}	SEA	192	789
Thermal losses, C_{therm}	PEA	21.5	193
Thermal losses, C_{therm}	SEA	37.8	703
Positive electrical work, C_{el}	PEA	7.80	103
Positive electrical work, C_{el}	SEA	186	797

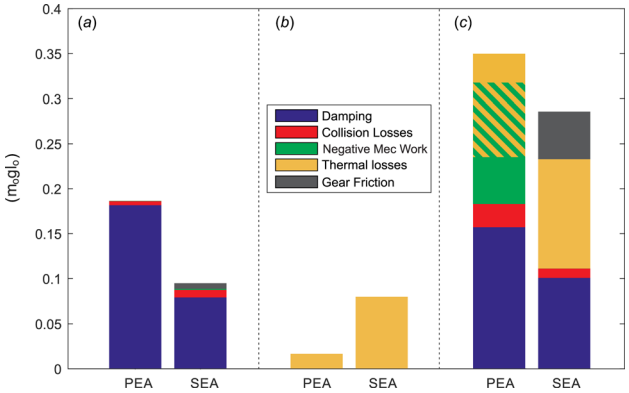

Fig. 6 Shown is the energetic breakdown for the three cost functions in the case of a rotary gearbox with friction and $n_\ell = 200\,\text{rad}/\ell_o$. Similar to the frictionless transmission case, for both C_{mech} and C_{el}, SEA was the energetically optimal actuator type. For C_{therm}, PEA was the optimal actuator type. For PEA, negative mechanical motor work compensated for a large proportion of the thermal losses (the cross-hatched region, indicating that though both losses occurred, they only were counted once): (*a*) C_{mech}, (*b*) C_{therm}, and (*c*) C_{el}.

torques from the motor are much smaller than for SEA, and there is, thus, no large penalty for using a smaller gearbox. Along the same lines of reasoning, SEA required a larger n to reduce the effective motor torque T_m and the associated thermal losses. Since leg motion and actuator motion were decoupled, there was no penalty for the resulting larger reflected rotor inertia.

For both actuation types, n was much smaller for the positive motor work cost function C_{mech} than for the other two cost functions. This result reflects again the fundamental differences that arise when considering C_{therm}. For C_{therm}, minimizing motor torques plays a more important role. Increasing n leads to smaller required T_m. This consideration is not important for C_{mech}, which is independent of n.

4.2 Rotary Gearbox With Friction, $n_\ell = 200\,\text{rad}/\ell_o$. Introducing friction in the transmission led to a new trade-off: in addition to creating a larger reflected rotor inertia, larger transmission ratios were now additionally penalized by larger friction values. For a rotary to linear transmission value of $n_\ell = 200\,\text{rad}/\ell_o$, this trade-off is not particularly grave.

As a result, the energetically optimal actuator type was cost function dependent in the same way as for the frictionless transmission (Fig. 6). For C_{mech}, the SEA hopper was 65% more

Table 3 Optimal stiffness and transmission values for the rotary gearbox with friction, n_ℓ=200 rad/ℓ_o case. Here, n is the overall transmission ratio ($n = n_r n_\ell$).

Cost function	Actuator type	k ($m_o g/\ell_o$)	n (rad/ℓ_o)
Positive motor work, C_{mech}	PEA	16.4	200
Positive motor work, C_{mech}	SEA	23.3	256
Thermal losses, C_{therm}	PEA	22.9	200
Thermal losses, C_{therm}	SEA	25.6	492
Positive electrical work, C_{el}	PEA	5.93	200
Positive electrical work, C_{el}	SEA	23.4	500

energetically economical than PEA (0.096 $m_o g\ell_o$ versus 0.19 $m_o g\ell_o$). For both actuators, energy was still primarily lost to damping, accounting for 84% of C_{mech} for SEA and 97% for PEA. Frictional losses in the gearbox were relatively low, as both actuators chose small optimal n_r values, which, therefore, had high efficiencies (Table 3). For SEA, the optimizer chose an overall transmission ratio of $n = 256\,\text{rad}/\ell_0$, while PEA had $n = 200\,\text{rad}/\ell_0$ (i.e., no rotary gearbox at all). As a result, for SEA, the frictional losses accounted only for 7% of the SEA losses and for none of the PEA losses. For C_{therm}, the PEA hopper was 131% more energetically economical than SEA (0.017 $m_o g\ell_o$ versus 0.080 $m_o g\ell_o$). For C_{el}, the SEA hopper was 20% more energetically economical than PEA (0.28 $m_o g\ell_o$ versus 0.35 $m_o g\ell_o$).

The results for the three cost functions followed the same general trend as in the completely frictionless transmission. The results held largely because of the advantage SEA obtains from utilizing a highly efficient rotary to linear transmission with a large transmission ratio. With the rotary to linear transmission doing most of the reduction ($n_l = 200\,\text{rad}/\ell_0$), only small values for n_r are necessary and there is a very small penalty for SEA to choose a large transmission ratio $n = n_l n_r$ (Eq. (17)). Therefore, the SEA costs showed only a slight increase due to gear friction. PEA, however, favored smaller transmission ratios for C_{mech} and C_{el}. Here, PEA attempted to have as low a transmission ratio as possible, choosing to have $n_r = 1$ for all cost functions. Still, with $n_l = 200\,\text{rad}/\ell_0$, it was forced to have a minimum transmission ratio that was larger than its optimal choice for the frictionless transmission. This nonoptimal choice of n drives up PEA costs for C_{mech} and C_{el} much higher than the slight gear friction for SEA, maintaining the trends from the frictionless transmission while increasing costs. In particular, for PEA, negative mechanical motor work became a significant portion of the C_{el} losses, likely

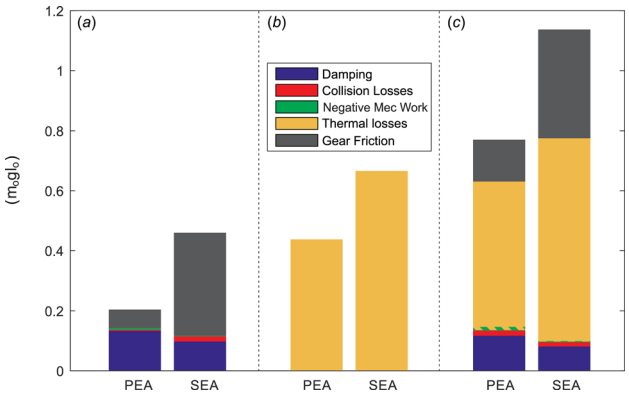

Fig. 8 The figure shows the energetic breakdown for the three cost functions in the case of a rotary gearbox with friction with $n_\ell = 2\,\text{rad}/\ell_o$. PEA was now optimal for all cost functions. The majority of the losses for C_{mech} arose from frictional and damping losses. For C_{el}, thermal losses and gear friction dominated the losses. (*a*) C_{mech}, (*b*) C_{therm}, and (*c*) C_{el}.

to avoid excess collisional losses from the larger transmission (Eq. (1)). For C_{therm}, the PEA cost and transmission ratio are nearly identical to the frictionless transmission.

For both PEA and SEA, the optimal motion was nearly identical to the frictionless transmission for C_{mech} and C_{therm} (Fig. 7). For C_{el}, there was again a trade-off between the oscillation strategy and the clamping strategy. The optimal C_{el} motion, however, changed. Whereas for the frictionless case, PEA chose the oscillation strategy, here it chose the clamping strategy. The consequences of the choice to suppress the natural oscillatory motion of the spring can be seen in the largely increased negative mechanical motor work for C_{el}.

4.3 Rotary Gearbox With Friction, n_ℓ=2 rad/ℓ_o. The rotary to linear transmission value of $n_\ell = 2\,\text{rad}/\ell_o$ in this case is relatively small. This case will, therefore, require substantially larger n_r values, which, in turn, will create larger friction losses.

This clearly benefited PEA, which was the energetically optimal actuator type for all cost functions in this case (Fig. 8). For C_{mech}, the PEA hopper was 77% more energetically economical than SEA (0.21 $m_o g\ell_o$ versus 0.46 $m_o g\ell_o$). For PEA, energy was primarily lost to damping, accounting for 65% of the losses. The frictional losses in the gearbox accounted for 30% of losses. For

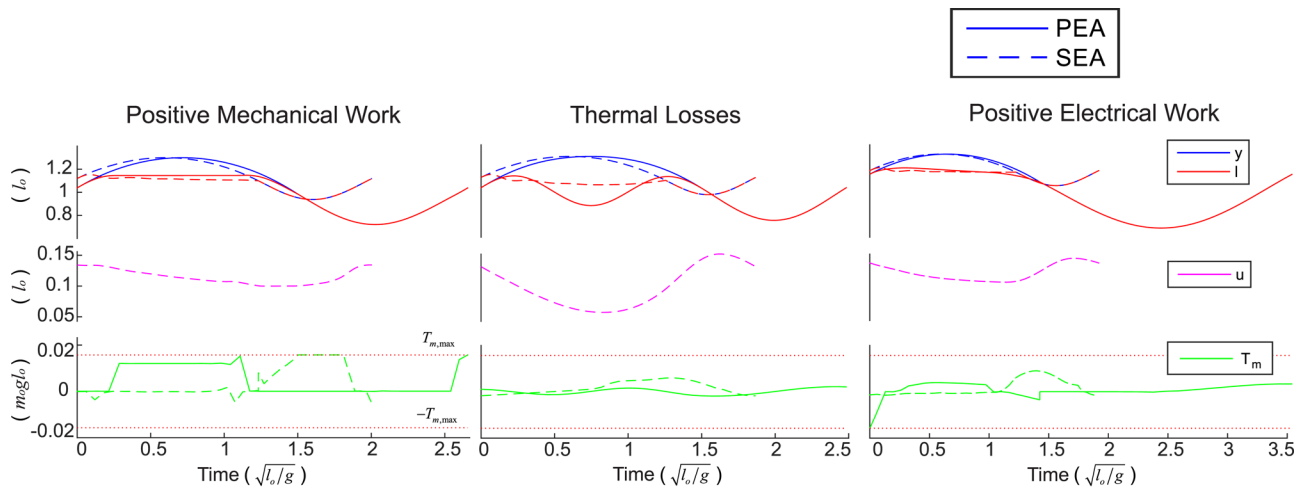

Fig. 7 Optimal motions and actuator inputs for the rotary gear box with friction and frictionless $n_\ell = 200\,\text{rad}/\ell_o$ case. Shown are the results for positive mechanical motor work (*a*), thermal losses (*b*), and electrical work (*c*). The most notable difference from the frictionless motion was that for PEA electrical work, it was no longer optimal to have the leg oscillate during flight. Instead, PEA and SEA adopted similar strategies during flight, holding their legs near maximum extension.

Table 4 Optimal stiffness and transmission values for the rotary gearbox with friction, frictionless n_ℓ=2 rad/ℓ_o case. Here, n is the overall transmission ratio ($n = n_r n_\ell$).

Cost function	Actuator type	k ($m_o g/\ell_o$)	n (rad/ℓ_o)
Positive motor work, C_{mech}	PEA	19.8	27.0
Positive motor work, C_{mech}	SEA	41.8	306
Thermal losses, C_{therm}	PEA	31.2	90
Thermal losses, C_{therm}	SEA	91.8	406
Positive electrical work, C_{el}	PEA	34.4	63.0
Positive electrical work, C_{el}	SEA	119	388

SEA, the trend was reversed: 75% was lost to gearbox friction, whereas 21% was lost to damping. For C_{therm}, the PEA hopper was 41% more energetically economical than SEA (0.44 $m_o g \ell_o$ versus 0.67 $m_o g \ell_o$). For C_{el}, the PEA hopper was 39% more energetically economical than SEA (0.77 $m_o g \ell_o$ versus 1.1 $m_o g \ell_o$). For both actuators, the losses were dominated by thermal losses and gear friction (Fig. 8).

In contrast to the previous cases, there was now a significant penalty for SEA to choose a large n, as it directly led to a large n_r and meant that there were significant frictional losses (Eq. (17)). PEA, with its smaller optimal rotary gearbox transmission n_r therefore suffered far lower frictional losses (Table 4).

The optimal motion for both PEA and SEA was now nearly identical for all three cost functions (Fig. 9). For all cost functions, both hoppers used the clamping strategy. There was no longer any oscillatory behavior by the PEA hopper. This lack of oscillatory behavior likely results from the presence of significant rotary gearbox friction. PEA could no longer choose as small of an n_r value as in the previous two cases, meaning that gear friction induced losses whenever the leg moved. Therefore, the optimizer chose to clutch the leg for all cost functions, avoiding unnecessary leg oscillation and removing any trade-off for C_{el}. C_{el} represented primarily the sum of C_{mech} and C_{therm}.

5 Discussion and Conclusions

In this study, we employed numerical optimization to compare optimal hopping motions of series and parallel elastic actuated hoppers. To make the comparison between the two actuation concepts as fair as possible, we compared the best possible hopper with SEA to the best possible hopper with PEA. To this end, we optimized actuator forces, motion trajectories, and system parameters simultaneously. The analysis was performed for three different cost functions: positive mechanical motor work C_{mech}, electrical thermal losses C_{therm}, and positive electrical work C_{el}. We studied hopping for two representative cases of rotary to linear transmission. In addition, we compared these results to an idealized case without friction in the transmission. Optimizing system parameters such as the rotary gearbox ratio and the stiffness of the springs was crucial. The different actuator types did require very different parameter values to perform optimally.

Given that C_{el} is the most complete cost function, we would conclude that for electrically driven hoppers, SEA is the most energetically economic actuator solution when the majority of the transmission ratio is accommodated for by a very high efficiency rotary to linear transmission, such as a prismatic ball screw. For a hopper with a smaller transmission (such as a robot hopping with a bent knee), however, PEA performed better. These optimal choices are primarily a consequence of the fact that SEA requires larger overall transmission ratios than PEA, as could be seen clearly when looking at the frictionless transmission. When the transmission ratios are achieved in an efficient way, SEA is the better actuator type. If they are subject to friction losses, PEA becomes the better actuator type.

Throughout our analysis, it became evident, that each configuration had a unique optimal motion profile and a set of parameters that differed greatly between the two actuation concepts. This clearly illustrated the necessity of our optimization approach. From a conceptual point of view, this simultaneous optimization of motion and morphology extends the paradigm of system-based design to include the future motion of the robotic system already at the design stage. We strongly believe that such a combined and simultaneous optimization of robot and motion will be at the core of future robotic design. This technique is slowly making its way into robotics, for example, in the optimization of an assistive device for sit-to-stand motions [41], to create stable running motions in a human-like robot [18] and to optimize limb lengths for particular tasks [19]. Here, we extended its principle to make a discrete design comparison between two fundamentally different morphologies. In the future, this approach can potentially be applied to more complex models and robots to achieve truly optimal performance during the design phase.

There are further important considerations for the actuator problem that must be explored before implementation in hardware. For PEA, the motor inertia is not isolated from collisions, which can lead to significant energetic losses. Therefore, it is imperative that the foot velocity is near-zero at touchdown. PEA achieves this by utilizing the oscillation strategy and clamping strategy, which let the spring passively retract the foot and minimize foot velocity with minimal energetic effect. Overall, we would argue that these optimal hopping strategies for PEA are

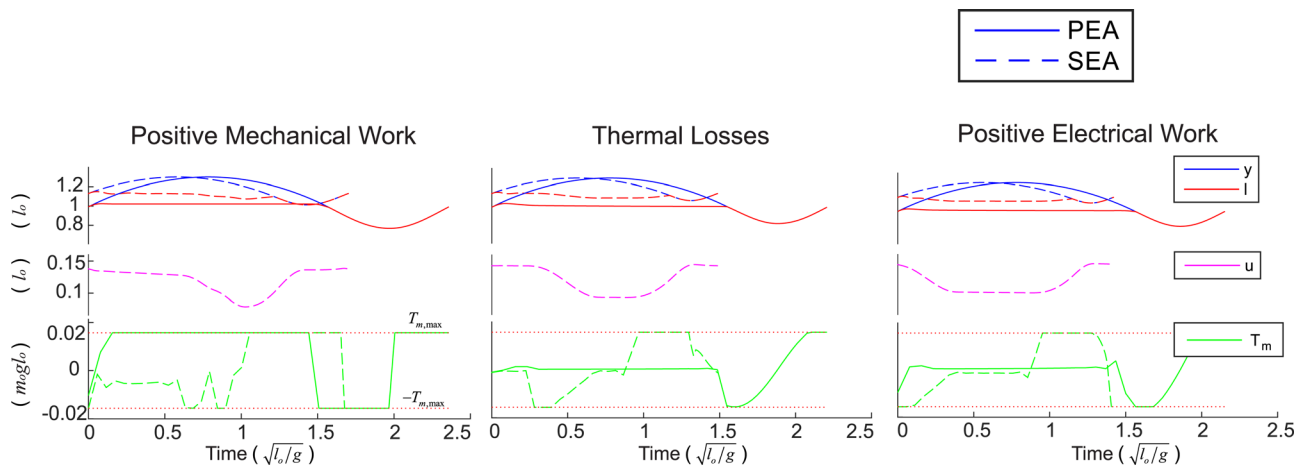

Fig. 9 Optimal motions and actuator inputs for the rotary gear box with friction and frictionless $n_\ell = 2$ rad/ℓ_o case. The motion here was very similar for both PEA and SEA for all three cost functions. Both hoppers extended their legs to near maximum extension during flight and held them there until touchdown.

more sensitive to timing issues and would be harder to implement in hardware. These strategies require a precise tuning of the spring stiffness, rotor inertia, and foot mass to achieve the correct spring natural frequency. However, small deviations from the optimal parameter values (e.g., caused by modeling errors or disturbances in the motion) can get in the way of this phase matching and might result in large collision losses.

In the present study, to avoid biasing the results toward either actuation configuration, we did not constrain the hopping frequency. The primary constraint on the hopping motion was that the hopper had to reach a height of $y = 1.3\ell_0$. This constraint ensured that the hoppers had both a stance phase and a flight phase. Timing was not considered, however, in finding the energetically optimal motion. From the motion plots, it is clear that SEA has significantly shorter optimal hopping periods, suggesting a potential advantage over PEA. In our prior work, the effect of frequency was implicitly included by enforcing an average velocity during two-dimensional motion [27] and was found to have little effect on the energetics at most speeds. Still, future studies could consider exploring hopping at a fixed frequency to see additional sensitivity effects.

There are additional mechanical and sensing complexities that must be taken into account when implementing either actuator type in hardware. For example, in PEA, the gearbox is not isolated from collisions. To prevent unnecessary damage to the gears, PEA would likely need an additional mechanism that softens these collisions. Furthermore, the spring could be disengaged to allow for easier leg retraction during swing. Karssen [16], for example, implements a clutch that disengages the spring during flight, and a small series elastic element that protects the gearbox. SEA would need additional components as well. Since SEA moves the proximal end of the spring, which, in turn, changes the leg length, it would need additional sensors to measure the location of each. More moving parts for SEA further means that additional bearings and mechanical components are necessary in practice.

Despite the simplicity of our models compared to a final hardware implementation, the motion strategies shown here can provide templates for further optimizations with more complex models and gaits. Given that hopping can be considered the archetype of legged locomotion [42,43], one would expect that similar motion patterns will be found in active running and walking gaits of multilegged robots. They can, thus, be used to systematically initialize optimizations or be employed as a tool to check the viability of more complex optimization results. This could enable roboticists to detect and avoid local minima that do not represent the global optimum in their optimizations. Finally, the actuation strategies that we observed in the optimal solutions provide an interesting departure point for further hardware development. For example, the clamping strategy that the optimizer discovered for PEA, where the leg was held fixed during the flight phase, could be implemented more efficiently with an actual clutch rather than with a DC motor.

The results presented in this work have been developed for the particular case of 1D hopping with electrically driven actuators. Certain parameters, such as the mass of the motors, are based off of our previous hardware [33]. The obtained motions, parameter choices, and cost values are specific to this choice of problem. From the work presented here, it is clear that even for this particular problem, the optimal actuation type is case dependent. It is impossible to state conclusively whether in general SEA or PEA is the better actuation concept for legged robots. Naturally, the cases presented in this work only represent a sample of a wide range of possible hopper configurations and focus on energetics. There likely is a gradual transition from hoppers, which would benefit from SEA to hoppers that should use PEA as friction in the transmission becomes more important. That is, ball screws are available with a wide variety of transmissions, knees can be operated at many different angles, and hybrids of the two transmission systems even exist [44]. Each of these transmission types can benefit a particular actuator. Additionally, more complexity has been introduced by robotic prototypes that utilize both SEA and PEA within a single design [16]. Future studies should take into account the vast variety of possible configurations.

The highly complex dependence on actuation type, parameters, and motion profile emphasizes the necessity of optimization to explore design issues. Still, it is important here to state that the methods we use are local, and so we are unable to guarantee their global optimality. In hopes of escaping local minima, all of the results presented in this paper represent optima that have been tested from a variety of different initial conditions.

Given that our evaluation took into account different cost functions that penalized force and work independently, our results can still be considered fairly general. Furthermore, this paper should also be understood as an introduction of a systematic methodology that enables a fair comparison of different robot morphologies. In a sense, the comparison of PEA and SEA is just an application of this method. In the future, this methodology can and should be extended to include other models as well as more complex motions. Moreover, the methodology can be utilized to look at other cost functions to maximize performance metrics other than energetics, such as maximizing hopping height.

Overall, the presented work gives a deeper understanding of the optimal motion for both SEA and PEA driven hopping motions. Understanding this underlying optimal motion can help designers ensure that they are not losing energy by unintentionally fighting the natural dynamics of a particular type of actuator. This understanding also gives insight into the coupling of morphology and motion. By using trajectory optimization, we can see how the choice of transmission ratio and stiffness change for a particular implementation and how these parameters and the resulting motion mutually influence each other. Recognizing these relationships opens the possibility to make robots more efficient, faster, and more robust.

Funding Data

- National Science Foundation (Grant No. 1453346).

References

[1] Alexander, R. M., 1990, "Three Uses for Springs in Legged Locomotion," Int. J. Rob. Res., **9**(2), pp. 53–61.

[2] Geyer, H., Seyfarth, A., and Blickhan, R., 2006, "Compliant Leg Behaviour Explains Basic Dynamics of Walking and Running," Proc. R. Soc. B, **273**(1603), pp. 2861–2867.

[3] Gan, Z., Wiestner, T., Weishaupt, M. A., Waldern, N. M., and Remy, C. D., 2015, "Passive Dynamics Explain Quadrupedal Walking, Trotting, and Tölting," ASME J. Comput. Nonlinear Dyn., **11**(2), p. 021008.

[4] Gan, Z., and Remy, C. D., 2014, "A Passive Dynamic Quadruped That Moves in a Large Variety of Gaits," IEEE/RSJ International Conference on Intelligent Robots and Systems (IROS 2014), Chicago, IL, Sept. 14–18, pp. 4876–4881.

[5] Cavagna, G. A., Heglund, N. C., and Taylor, C. R., 1977, "Mechanical Work in Terrestrial Locomotion: Two Basic Mechanisms for Minimizing Energy Expenditure," Am. J. Physiol.: Regul., Integr. Comp. Physiol., **233**(5), pp. R243–R261.

[6] Blickhan, R., 1989, "The Spring-Mass Model for Running and Hopping," J. Biomech., **22**(11–12), pp. 1217–1227.

[7] Lichtwark, G. A., and Wilson, A. M., 2005, "In Vivo Mechanical Properties of the Human Achilles Tendon During One-Legged Hopping," J. Exp. Biol., **208**(24), pp. 4715–4725.

[8] Dean, J. C., and Kuo, A. D., 2011, "Energetic Costs of Producing Muscle Work and Force in a Cyclical Human Bouncing Task," J. Appl. Physiol., **110**(4), pp. 873–880.

[9] Alexander, R. M., 1992, "A Model of Bipedal Locomotion on Compliant Legs," Philos. Trans. R. Soc. London. Ser. B, **338**(1284), pp. 189–198.

[10] Xi, W., and Remy, C. D., 2014, "Optimal Gaits and Motions for Legged Robots," IEEE/RSJ International Conference on Intelligent Robots and Systems (IROS 2014), Chicago, IL, Sept. 14–18, pp. 3259–3265.

[11] Pratt, G. A., and Williamson, M. M., 1995, "Series Elastic Actuators," IEEE/RSJ International Conference on Human Robot Interaction and Cooperative Robots. Intelligent Robots and Systems 95, Pittsburgh, PA, Aug. 5–9, pp. 399–406.

[12] Hurst, J., and Rizzi, A., 2008, "Series Compliance for an Efficient Running Gait," IEEE Rob. Autom. Mag., **15**(3), pp. 42–51.

[13] Hutter, M., Remy, C. D., and Siegwart, R., 2009, "Design of an Articulated Robotic Leg With Nonlinear Series Elastic Actuation," International Conference on CLimbing and WAlking Robots (CLAWAR), Istanbul, Turkey, Sept. 9–11, pp. 645–652.

[14] Seyfarth, A., Iida, F., Tausch, R., Stelzer, M., von Stryk, O., and Karguth, A., 2009, "Towards Bipedal Jogging as a Natural Result of Optimizing Walking Speed for Passively Compliant Three-Segmented Legs," Int. J. Rob. Res., **28**(2), pp. 257–265.
[15] Paine, N., Oh, S., and Sentis, L., 2014, "Design and Control Considerations for High-Performance Series Elastic Actuators," IEEE/ASME Trans. Mechatronics, **19**(3), pp. 1080–1091.
[16] Karssen, J., 2013, "Robotic Bipedal Running: Increasing Disturbance Rejection," Ph.D. thesis, Delft University of Technology, Delft, The Netherlands.
[17] Grizzle, J., Hurst, J., Morris, B., Park, H.-W., and Sreenath, K., 2009, "MABEL, a New Robotic Bipedal Walker and Runner," American Control Conference (ACC'09), St. Louis, MO, June 10–12, pp. 2030–2036.
[18] Mombaur, K., 2009, "Using Optimization to Create Self-Stable Human-Like Running," Robotica, **27**(3), pp. 321–330.
[19] Ha, S., Coros, S., Alspach, A., Kim, J., and Yamane, K., 2016, "Task-Based Limb Optimization for Legged Robots," IEEE/RSJ International Conference on Intelligent Robots and Systems (IROS), Daejeon, South Korea, Oct. 9–14, pp. 2062–2068.
[20] Geijtenbeek, T., van de Panne, M., and van der Stappen, A. F., 2013, "Flexible Muscle-Based Locomotion for Bipedal Creatures," ACM Trans. Graph., **32**(6), p. 206.
[21] Paul, C., and Bongard, J. C., 2001, "The Road Less Travelled: Morphology in the Optimization of Biped Robot Locomotion," IEEE/RSJ International Conference on Intelligent Robots and Systems, Maui, HI, Oct. 29–Nov. 3, pp. 226–232.
[22] Cao, Q., and Poulakakis, I., 2014, "On the Energetics of Quadrupedal Bounding With and Without Torso Compliance," IEEE/RSJ International Conference on Intelligent Robots and Systems (IROS 2014), Chicago, IL, Sept. 14–18, pp. 4901–4906.
[23] James, J., Ross, P., and Ball, D., 2015, "Comparison of Elastic Configurations for Energy Efficient Legged Locomotion," Australasian Conference on Robotics and Automation, Canberra, Australia, Dec. 2–4.
[24] Grimmer, M., Eslamy, M., Gliech, S., and Seyfarth, A., 2012, "A Comparison of Parallel- and Series Elastic Elements in an Actuator for Mimicking Human Ankle Joint in Walking and Running," IEEE International Conference on Robotics and Automation (ICRA), Saint Paul, MN, May 14–18, pp. 2463–2470.
[25] Blickhan, R., and Full, R., 1993, "Similarity in Multilegged Locomotion: Bouncing Like a Monopode," J. Comp. Physiol. A, **173**(5), pp. 509–517.
[26] Yesilevskiy, Y., Xi, W., and Remy, C. D., 2015, "A Comparison of Series and Parallel Elasticity in a Monoped Hopper," IEEE International Conference on Robotics and Automation (ICRA), Seattle, WA, May 26–30, pp. 1036–1041.
[27] Yesilevskiy, Y., Gan, Z., and Remy, C. D., 2016, "Optimal Configuration of Series and Parallel Elasticity in a 2D Monoped," IEEE International Conference on Robotics and Automation (ICRA), Stockholm, Sweden, May 16–21, pp. 1360–1365.
[28] Remy, C. D., Buffinton, K., and Siegwart, R., 2012, "Comparison of Cost Functions for Electrically Driven Running Robots," IEEE International Conference on Robotics and Automation (ICRA), Saint Paul, MN, May 14–18, pp. 2343–2350.
[29] Karssen, J., and Wisse, M., 2012, "Running Robot Phides," Dynamic Walking Conference, Hilton, FL, May 21–25.
[30] Laughton, M. A., and Warne, D., 2002, *Electrical Engineer's Reference Book*, Newnes, London.
[31] Thomson, 2016, "Lead Screws, Ball Screws, and Ball Splines Catalog," Thomson Industries, Inc., Radford, VA, accessed Mar. 15, 2018, https://www.thomsonlinear.com/downloads/screws/Leadscrews_Ballscrews_Splines_cten.pdf
[32] Maxon Motor, 2010/2011, "Maxon Program 2010/2011," Maxon Motor, Sachseln, Switzerland, accessed Mar. 15, 2018, https://www.maxonmotor.nl/maxon/view/news/MEDIENMITTEILUNG-Programm-2010-Katalog?isoCode=fr
[33] Hutter, M., Remy, C. D., Hoepflinger, M. A., and Siegwart, R., 2011, "Scarleth: Design and Control of a Planar Running Robot," IEEE/RSJ International Conference on Intelligent Robots and Systems (IROS), San Francisco, CA, Sept. 25–30, pp. 562–567.
[34] Bock, H. G., and Plitt, K.-J., 1984, "A Multiple Shooting Algorithm for Direct Solution of Optimal Control Problems," IFAC Proc., **17**(2), pp. 1603–1608.
[35] Leineweber, D., 1999, *Efficient Reduced SQP Methods for the Optimization of Chemical Processes Described by Large Sparse DAE Models*, VDI-Verlag, Düsseldorf, Germany.
[36] Diehl, M., Leineweber, D. B., and Schäfer, A. A., 2001, *MUSCOD-II User's Manual*, IWR, Berlin.
[37] Srinivasan, M., and Ruina, A., 2006, "Computer Optimization of a Minimal Biped Model Discovers Walking and Running," Nature, **439**(7072), pp. 72–75.
[38] Remy, C. D., 2011, "Optimal Exploitation of Natural Dynamics in Legged Locomotion," Ph.D. thesis, Eidgenössische Technische Hochschule, Zürich, Switzerland.
[39] Srinivasan, M., 2011, "Fifteen Observations on the Structure of Energy-Minimizing Gaits in Many Simple Biped Models," J. R. Soc. Interface, **8**(54), pp. 74–98.
[40] Rebula, J. R., and Kuo, A. D., 2015, "The Cost of Leg Forces in Bipedal Locomotion: A Simple Optimization Study," PLoS One, **10**(2), p. e0117384.
[41] Hoang, K.-L. H., and Mombaur, K. D., 2015, "Optimal Design of a Physical Assistive Device to Support Sit-to-Stand Motions," IEEE International Conference on Robotics and Automation (ICRA), Seattle, WA, May 26–30, pp. 5891–5897.
[42] Raibert, M. H., Brown, H. B., and Chepponis, M., 1984, "Experiments in Balance With a 3D One-Legged Hopping Machine," Int. J. Rob. Res., **3**(2), pp. 75–92.
[43] Koepl, D., and Hurst, J., 2011, "Force Control for Planar Spring-Mass Running," IEEE/RSJ International Conference on Intelligent Robots and Systems (IROS), San Francisco, CA, Sept. 25–30, pp. 3758–3763.
[44] Pratt, J., and Krupp, B., 2008, "Design of a Bipedal Walking Robot," SPIE Defense and Security Symposium, Orlando, FL, Mar. 16–20, p. 69621F.